THE JOURNAL OF BIOLOGICAL CHEMISTRY VOL. 285, NO. 19, pp. 14639–14647, May 7, 2010

Dynamic Effects of Cofactors and DNA on the Oligomeric State of Human Mitochondrial DNA Helicase*[S]

Received for publication, December 28, 2009, and in revised form, February 17, 2010 Published, JBC Papers in Press, March 8, 2010, DOI 10.1074/jbc.M109.099663

Tawn D. Ziebarth[‡1], Rocio Gonzalez-Soltero[§1], Magdalena M. Makowska-Grzyska[‡1], Rafael Núñez-Ramírez[§2], Jose-Maria Carazo[§], and Laurie S. Kaguni[‡3]

From the [‡]Department of Biochemistry and Molecular Biology and the Center for Mitochondrial Science and Medicine, Michigan State University, East Lansing, Michigan 49924-1319 and the [§]Centro Nacional de Biotecnología Consejo Superior de Investigaciones Cientificas (CSIC), Unidad de Biocomputación, Cantoblanco, 28049 Madrid, Spain

We examined the effects of cofactors and DNA on the stability, oligomeric state and conformation of the human mitochondrial DNA helicase. We demonstrate that low salt conditions result in protein aggregation that may cause dissociation of oligomeric structure. The low salt sensitivity of the mitochondrial DNA helicase is mitigated by the presence of magnesium, nucleotide, and increased temperature. Electron microscopic and glutaraldehyde cross-linking analyses provide the first evidence of a heptameric oligomer and its interconversion from a hexameric form. Limited proteolysis by trypsin shows that binding of nucleoside triphosphate produces a conformational change that is distinct from the conformation observed in the presence of nucleoside diphosphate. We find that single-stranded DNA binding occurs in the absence of cofactors and renders the mitochondrial DNA helicase more susceptible to proteolytic digestion. Our studies indicate that the human mitochondrial DNA helicase shares basic properties with the SF4 replicative helicases, but also identify common features with helicases outside the superfamily, including dynamic conformations similar to other AAA$^+$ ATPases.

The human mitochondrial DNA (mtDNA)[4] helicase represents the most recent addition to the mitochondrial replication fork. This novel enzyme has been classified as an *Escherichia coli* (*E. coli*) DnaB-like replicative helicase (or SF4 replicative helicase) (1). Members of SF4 were first identified in bacteria and bacteriophages. Proteins within the SF4 family possess an N-terminal primase-interacting domain (in the case of *E. coli* DnaB) or primase domain (in the case of bacteriophage T7 gene 4 protein, T7 gp4). The human mtDNA helicase is capable of hydrolyzing nucleotides to provide energy for DNA translocation and duplex unwinding (2). As purified at 330 mM NaCl, its native molecular weight is consistent with that of a hexameric quaternary structure, which is believed to be its active conformation during translocation, similar to various eukaryotic and prokaryotic helicases (1).

The bacteriophage T7 gp4 protein exists predominantly in the hexameric state, yet both a crystal structure and electron microscopic images demonstrate a heptameric oligomer either in the absence of cofactors, or in the presence of Mg^{2+}-dTDP (3, 4). Furthermore, Richardson *et al.* (5) recently showed that the type of nucleotide present, di- or triphosphate, is detected by a phosphate sensor at histidine 465 that dictates a conformational switch from the heptameric to hexameric state, respectively. The T7 enzyme is not unique in this aspect as the *Methanobacterium thermoautotrophicum* minichromosomal maintenance protein (*mt*MCM) and the *Thermus thermophilus* HB8 RuvB protein also exist as heptamers, both of which are members of the SF6 family (6, 7). The SF6 helicase family comprises a divergent group of proteins that contain an N-terminal DNA-interacting domain and a C-terminal helix-turn-helix motif, which are not present in proteins from SF4 (8). Although the physiological role for the heptameric conformation has yet to be established, it is clear that the state is regulated by environmental conditions.

Increasing temperature has been shown to stabilize the *E. coli* DnaB protein (9). Furthermore, Liu *et al.* demonstrated that the presence of nucleotide drives the bacteriophage T4 gene 41 protein dimer to a higher oligomeric state (10). Hydrodynamic studies of *E. coli* DnaB reveal that the presence of Mg^{2+}, nucleotide or increasing salt induces the dimerization of trimers into a hexameric form, whereas electron microscopic images suggest a trimerization of dimers (11–13). T7 gp4 has been shown to exist as a dimer and trimer that oligomerize into hexamers in the presence of dTTP, but in the absence of Mg^{2+} (14–16). Although all of these proteins are members of the same superfamily, different nucleotide requirements for achieving an active oligomeric state most likely serve a regulatory role that is specific to the given organism.

The binding of cofactors to helicases not only induces oligomerization of the enzymes into a stable, active state, it also brings about a conformational change that is necessary for its function during replication. Limited proteolysis of *E. coli* DnaB protein shows a conformational change upon nucleotide binding (17). Similar findings reported by Romano *et al.* (18) illus-

* This work was supported, in whole or in part, by Grant GM45295 from the National Institutes of Health (to L. S. K.). This work was also supported by Grants CSD2006-00023 and BIO2007-67150-C03-1 from MEC and S-GEN-0166-2006 from CAM (to J.-M. C.).

[S] The on-line version of this article (available at http://www.jbc.org) contains supplemental Figs. S1–S3.

[1] These authors contributed equally to this work.

[2] Present address: Departamento de Física Macromolecular, Instituto de Estructura de la Materia, CSIC Serrano 113 bis, 28006 Madrid, Spain.

[3] To whom correspondence should be addressed. Tel.: 517-353-6703; Fax: 517-353-9334; E-mail: lskaguni@msu.edu.

[4] The abbreviations used are: mtDNA, mitochondrial DNA; T7 gp4, bacteriophage T7 gene 4 protein; *mt*MCM, *M. thermoautotrophicum* minichromosomal maintenance protein; ssDNA, single-stranded DNA; ATPγS, adenosine 5′-[γ-thio] triphosphate; His, hexahistidine; ML2D, maximum likelihood 2D; SOM, self-organizing maps; CL2D, clustering 2D.

trate numerous conformations of T7 gp4 in the presence of various nucleotides and DNA. These conformations are presumed to facilitate nucleotide hydrolysis and the mechanism of single-stranded DNA (ssDNA) translocation that leads to double-stranded DNA (dsDNA) unwinding.

A fundamental property required of all replicative helicases is the ability to bind to ssDNA. A crystal structure of T7 gp4 confirmed electron microscopic studies by showing that C-terminal domain loops projecting into the center of the ring are responsible for ssDNA binding (19–21). The ability of T7 gp4 to bind to DNA is dependent on its hexameric form and the binding of nucleotides as shown for *E. coli* DnaB (16, 22, 23). *Mt*MCM, on the other hand, binds DNA in the absence of nucleotide as a double hexamer (24).

We explored some basic characteristics of the human mtDNA helicase by investigating aspects common to *E. coli* DnaB-like helicases and helicases that lie outside of this family of enzymes. We examined factors stabilizing the human mtDNA helicase under physiological ionic conditions, and found that nucleotide is required for the retention of a soluble, stable protein in a low ionic environment. We also examined oligomeric state and conformational changes under the stabilizing conditions, using hydrodynamic, electron microscopic and biochemical methods. Our study reveals dynamic features of the human mtDNA helicase that suggest the possibility of multiple levels of regulated interactions in its role in mtDNA replication.

EXPERIMENTAL PROCEDURES

Materials

Trypsin, soybean trypsin inhibitor, and ATPγS were purchased from Sigma. Calf thymus DNA (highly polymerized Type I) was purchased from Sigma and was activated by partial digestion with DNase I (Roche Applied Science). Sodium dodecyl sulfate (SDS) was from Pierce. Nitrocellulose membranes were purchased from DOT Scientific, Inc. Rabbit antisera raised against recombinant human mtDNA helicase was prepared as described by Wang *et al.* (25). Alkaline phosphatase-conjugated anti-rabbit IgG was purchased from Bio-Rad.

Methods

Protein Overexpression and Purification of Human mtDNA Helicase—N- and C-terminally hexahistidine (His)-tagged human mtDNA helicase was produced by overexpression in *Spodoptera frugiperda* cells and purified to homogeneity, as described in Ziebarth *et al.* (1). Both N-and C-terminally tagged helicase were tested in all of the experiments shown in this report (stability, glutaraldehyde cross-linking, sedimentation, gel filtration, electron microscopy, and proteolysis), and we found no differences in the results based on the placement of the tag. Furthermore, we demonstrated in Ziebarth *et al.* (1) that the placement of the tag at either end affects neither the oligomerization properties nor the ATPase activity of the human mtDNA helicase.

Solubility Assay—Reaction mixtures (25 μl) contained 35 mM Tris-HCl, pH 7.5, 0.1 mM EDTA, and N-terminally His-tagged human mtDNA helicase (Fr IV; 1.25 μg, 0.12 μM as hexamer) in the absence or presence of 4 mM $MgCl_2$, 2 mM ADP, 2 mM ATP, or 2 mM ATPγS as indicated. Incubation was for 1 h at 4, 24 or 37 °C followed by centrifugation at 10,000 × *g* for 10 min. Soluble and insoluble fractions were made 1% in SDS, heated for 2 min at 100 °C and electrophoresed in a 10% SDS-polyacrylamide gel according to Laemmli (26). Protein bands were visualized by silver staining. The data were photographed and quantitated using Kodak 1D software.

Cross-linking Analysis of the Human mtDNA Helicase—Reaction mixtures (50 μl) contained 5 mM Tris-HCl, pH 7.5, 100 mM NaCl, 0.1 mM EDTA, 1 mM dithiothreitol, and 50 μg/ml of N-terminally His-tagged human mtDNA helicase (Fr IV; 2.5 μg, 0.12 μM as hexamer). Samples were incubated for 30 min at 37 °C in the absence or presence of four cofactors: 4 mM $MgCl_2$, 2 mM ADP, 2 mM ATP, or 2 mM ATPγS and heated DNA oligomer (75 mer) as indicated. Following the incubation, cross-linking with 0.02% glutaraldehyde was performed for 20 min at 37 °C. The reactions were quenched with 200 μl of 10 mM Tris-HCl, pH 8.0, 1 mM EDTA followed by precipitation with trichloroacetic acid using 2 μg of cytochrome *c* as a carrier. Cross-linked products were separated by SDS-PAGE in a 3.5% polyacrylamide gel. Proteins were transferred to nitrocellulose membranes and probed by immunoblotting.

Analytical Velocity Sedimentation of Human mtDNA Helicase—N- and C-terminally His-tagged human mtDNA helicase (FrIV; 40 μg, 0.12 μM as hexamer) was layered onto preformed 12–30% glycerol gradients (10 ml) containing 35 mM Tris-HCl, pH 7.5, 330 or 100 mM NaCl, 1 mM phenylmethylsulfonyl fluoride, 10 mM sodium metabisulfite, 2 μg/ml leupeptin, and 10 mM 2-mercaptoethanol. Helicase was incubated for 30 min at 24 °C in the absence or presence of 4 mM $MgCl_2$ and 2 mM ATPγS. Protein standards of known S values run in parallel were: jack bean urease, 18.6 S; bovine liver catalase, 11.3 S; rabbit muscle L-lactate dehydrogenase, 7.3 S. Centrifugation was at 37,000 rpm for 15 h at 4 °C in a Beckman SW 41 rotor. Fractions were precipitated with trichloroacetic acid and analyzed by SDS-PAGE followed by silver staining.

Gel Filtration of Human mtDNA Helicase at 330 mM NaCl—C-terminally His-tagged human mtDNA helicase (180 μg, 0.35 mg/ml) was chromatographed on a Superdex 200 HR 10/30 column (10 mm × 300–310 mm, Amersham Biosciences) equilibrated with buffer containing 35 mM Tris-HCl, pH 7.5, 330 mM NaCl, 8% glycerol, 0.5 mM EDTA, and 0.02% (v/v) *n*-dodecyl-β-D-maltopyranoside at a flow rate of 0.25 ml/min at 4 °C. The column was calibrated with chymotrypsinogen A (R_s = 28 Å), hen egg ovalbumin (R_s = 30 Å), yeast alcohol dehydrogenase (R_s = 46 Å), bovine liver catalase (R_s = 52 Å) and bovine thyroid thyroglobulin (R_s = 85 Å), where R_s is the Stoke's radius. Fractions (0.25 ml) were collected, and aliquots were analyzed by SDS-PAGE and Coomassie staining to confirm ultraviolet trace recordings.

Gel Filtration of Human mtDNA Helicase at 100 mM NaCl in the Presence of Cofactors—C-terminally His-tagged human mtDNA helicase was diluted in a buffer containing Tris-HCl, pH 7.5, ATPγS, $MgCl_2$ and *n*-dodecyl-β-D-maltopyranoside to achieve final concentrations of 2 mM ATPγS, 4 mM $MgCl_2$, 0.02% *n*-dodecyl-β-D-maltopyranoside, and 100 mM NaCl. The sample was incubated at 37 °C for 10 min, chilled to 0 °C, and centrifuged at 10,000 × *g* for 5 min. The supernatant fraction

(180 μg, 0.18 mg/ml) was chromatographed on a Superdex 200 HR 10/30 column equilibrated with buffer containing 35 mM Tris-HCl, pH 7.5, 100 mM NaCl, 0.5 mM EDTA, 8% glycerol, 2 mM ATP, 4 mM $MgCl_2$, 0.02% *n*-dodecyl-β-D-maltopyranoside at a flow rate of 0.25 ml/min at 4 °C. Fractions (0.25 ml) were analyzed as described above.

Electron Microscopy and Image Processing—Protein samples were adsorbed directly onto carbon/collodion-coated copper grids that had been glow discharged. Following negative staining with 2% (w/v) uranyl acetate, the samples were visualized in a JEOL JEM-1011 electron microscope. Micrographs were taken at a magnification of 50,000× and scanned in a Zeiss scanner resulting in a final pixel size of 4.2 A/pixels in the object scale. Image processing analysis was carried out using the XMIPP package (27, 28). Two-dimensional alignment and heterogeneity analysis were performed using several classification algorithms: maximum likelihood (29), self-organizing map of rotational spectra (30) and clustering two-dimensional CL2D, a new multireference classification algorithm using correntropy, divisive clustering and a new clustering criterion to split the original dataset into disjoint classes.[5] The algorithm refine2d.py from the EMAN package was used for the 330 mM NaCl samples (31).

Protein Immunoblotting—Nitrocellulose membranes were preincubated for 1 h in 20 mM Tris-HCl, pH 7.5, 150 mM NaCl, 0.05% (v/v) Tween 20 (TBST), and 5% (w/v) nonfat milk. The membranes were probed with human mtDNA helicase antibody (1:100 in TBST and 1% nonfat milk), for 2 h and then washed three times for 5 min each with TBST. After the washes were complete, incubation for 1 h was performed with goat anti-rabbit IgG alkaline phosphatase conjugate (1:1500 (v/v) in TBST with 1% nonfat milk), and then the membranes were washed three times for 5 min with TBST, and once for 5 min in 100 mM Tris-HCl, pH 9.5, 100 mM NaCl and 5 mM $MgCl_2$ (alkaline phosphatase buffer). The membranes were developed by incubation in alkaline phosphatase buffer containing nitro blue tetrazolium (330 μg/ml) and 5-bromo-4-chloro-3-indolyl phosphate (165 μg/ml).

Trypsin Digestion—Reaction mixtures (30 μl) contained 35 mM Tris-HCl, pH 7.5, 100 mM NaCl, 1 mM dithiothreitol, and N-terminally His-tagged human mtDNA helicase (FrIV; 1.5 μg, 0.12 μM as hexamer). The reactions were incubated for 30 min at 24 °C in the absence or presence of 4 mM $MgCl_2$, 2 mM ADP, 2 mM ATP, or 2 mM ATPγS as indicated. In the experiment shown in Fig. 7, reactions contained 0.25 μM heat-denatured, DNaseI-activated calf thymus DNA. In the experiment shown in Fig. 8, reactions contained 0.1, 0.4, and 2 μM heat-denatured, DNaseI-activated calf thymus DNA as indicated. Trypsin was added to reactions at a helicase: trypsin ratio of 1:1 unless indicated otherwise, followed by incubation for 10 min at 24 °C. Digestions were stopped by the addition of soybean trypsin inhibitor at a trypsin:soybean trypsin inhibitor ratio of 1:2. Digestion products were separated by SDS-PAGE, and analyzed by silver staining.

[5] Sorzano, C. O., Bilbao-Castro, J. R., Shkolnisky, Y., Alcorlo, M., Melero, R., Caffarena-Fernández, G., Li, M., Xu, G., Marabini, R., and Carazo, J. M. (2010) *J. Struct. Biol.*, in press.

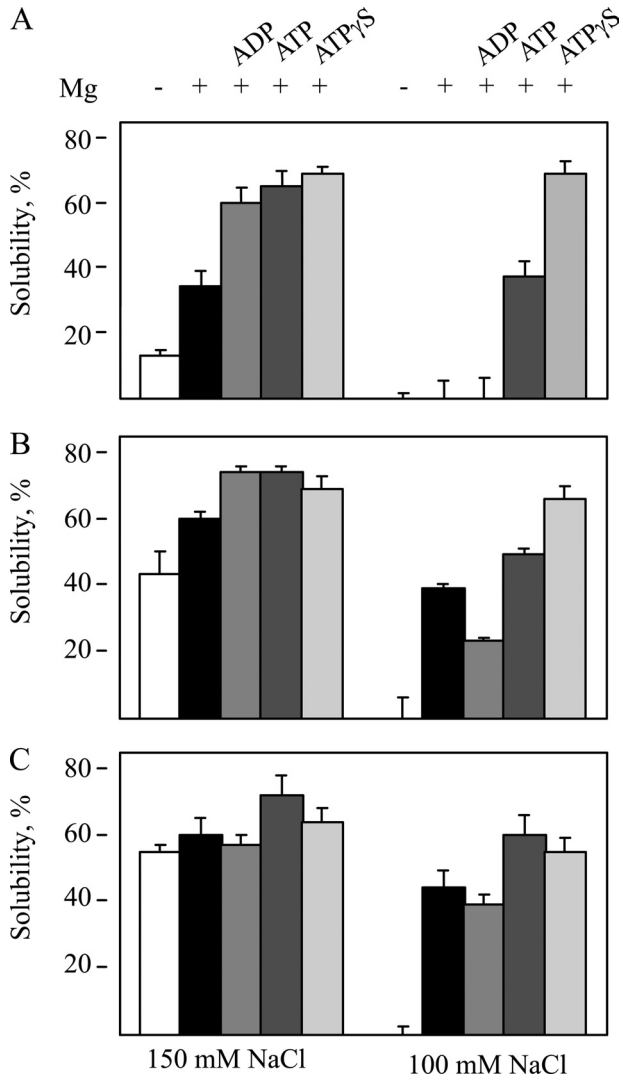

FIGURE 1. **Factors stabilizing the human mtDNA helicase under physiological ionic conditions.** N-terminally His-tagged human mtDNA helicase was incubated at 150 mM and 100 mM NaCl in the absence (*white bars*) and presence of Mg^{2+} (*black bars*), Mg^{2+}-ADP (*medium gray bars*), Mg^{2+}-ATP (*dark gray bars*), Mg^{2+}-ATPγS (*light gray bars*), and subjected to centrifugation as described under "Experimental Procedures." Aliquots of soluble factions at 4 °C (*A*), 24 °C (*B*), and 37 °C (*C*) were analyzed by SDS-PAGE followed by silver staining. Error bars represent standard deviation among duplicate samples from each of four independent experiments.

Other Methods—Gel electrophoresis and protein transfer were performed as described by Wang *et al.* (25).

RESULTS

Factors Stabilizing the Human mtDNA Helicase under Physiological Ionic Conditions—The recombinant human mtDNA helicase is a soluble, stable enzyme at 330 mM NaCl (1). However, solubility is decreased dramatically when the salt concentration is reduced to the physiological range, either by simple dilution or dialysis. To identify factors that might stabilize the enzyme at moderate (150 mM NaCl) and low (100 mM NaCl) salt concentrations, we incubated the protein at different temperatures under various conditions, and examined its stability by evaluating recovery in the soluble fraction following centrifugation (see "Experimental Procedures"). In the absence of Mg^{2+} or nucleotide at moderate salt, increased temperatures in the

range of 4−37 °C enhance the recovery of soluble protein whereas at low salt, we observe complete insolubility (Fig. 1, *A–C*). With increased temperatures, the presence of Mg^{2+} increases the solubility of the enzyme at both salt concentrations, and stability is increased further with the addition of ATP. ADP appears to have no significant effect. At low ionic strength, we found the greatest effect of temperature on solubility in the presence of Mg^{2+} and the non-hydrolyzable ATP analogue, ATPγS. Together the results indicate that in a physiological ionic environment, the human mtDNA helicase is most stable when nucleoside triphosphate is bound but not hydrolyzed.

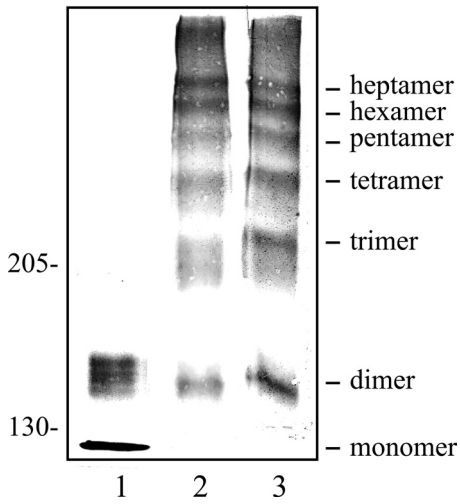

FIGURE 2. **Oligomeric states of the human mtDNA helicase in the presence of cofactors and DNA substrate.** N-terminally His-tagged human mtDNA helicase was preincubated under the indicated conditions for 30 min at 37 °C prior to cross-linking with 0.02% glutaraldehyde for 20 min at 37 °C. Samples were analyzed by SDS-PAGE followed by immunoblotting. *Lane 1*, absence of cofactors and glutaraldehyde; *lane 2*, Mg^{2+}-ATPγS; *lane 3*, Mg^{2+}-ATPγS-DNA (75-mer).

Oligomeric States of the Human mtDNA Helicase in the Presence of Cofactors and DNA Substrate—To investigate the oligomeric state of the human mtDNA helicase in the presence or absence of cofactors and DNA under low salt conditions, we used glutaraldehyde cross-linking followed by SDS-PAGE (see "Experimental Procedures" and Fig. 2). In the absence of glutaraldehyde and cofactors (*lane 1*), we observed predominantly monomers but also a stable dimeric form of the protein that is resistant to denaturing conditions. The addition of glutaraldehyde in the absence of cofactors also yields only soluble monomers and dimers, but results in an increase in aggregation that promotes protein loss, which is consistent with the results we obtained in the solubility assay. In contrast, the inclusion of both Mg^{2+} and ATP or ATPγS prior to cross-linking results in a decrease in aggregation and an increase in protein recovery, again consistent with the solubility assay. Here we observe oligomeric species ranging from dimers to hexamers, and demonstrate for the first time a heptameric form of the human protein (*lane* 2). Based on our earlier hydrodynamic studies, the starting material is expected to be hexameric (not distinguishing hexamers/heptamers, (1)), so it is likely that the smaller species observed in this analysis result from incompletely cross-linked hexamers/heptamers. The presence of DNA in glutaraldehyde cross-linking, either in the presence or absence of cofactors under the various reactions described in Fig. 1, shows no effect on the oligomeric state of the enzyme (*lane* 3). We examined further the effects of cofactors using velocity sedimentation. As we observed previously (1), the mtDNA helicase sediments in high yield in a single peak in the presence of 330 mM NaCl, with a sedimentation coefficient of 13.7 S (Fig. 3). Sedimentation of the enzyme under low salt conditions (100 mM NaCl) in the absence of cofactors resulted in very poor yields, with insoluble, aggregated material found in the gradient pellet (data not shown). However, inclusion of Mg^{2+} and ATPγS reproducibly results in the appearance of a single peak with a sedimentation coefficient of 16.1 S. Similarly, gel filtration of the enzyme at 330 mM NaCl produces a single peak with a Stokes radius of 80 Å. Gel filtration at 100 mM NaCl and in the presence of Mg^{2+} and ATPγS results in a single peak with a Stokes radius of 84 Å (Fig. 3). Combining the sedimentation coefficient with the Stokes radius for the enzyme at 330 mM NaCl yields a native molecular mass of 427,000 daltons that is similar to the value previously reported (1). The same calculation performed for the mtDNA helicase in the presence of 100 mM NaCl, Mg^{2+}, and ATPγS gives a native molecular mass of 528,000 daltons. The combined increases in sedimentation coefficient and Stokes radius suggest that the protein exists in a different

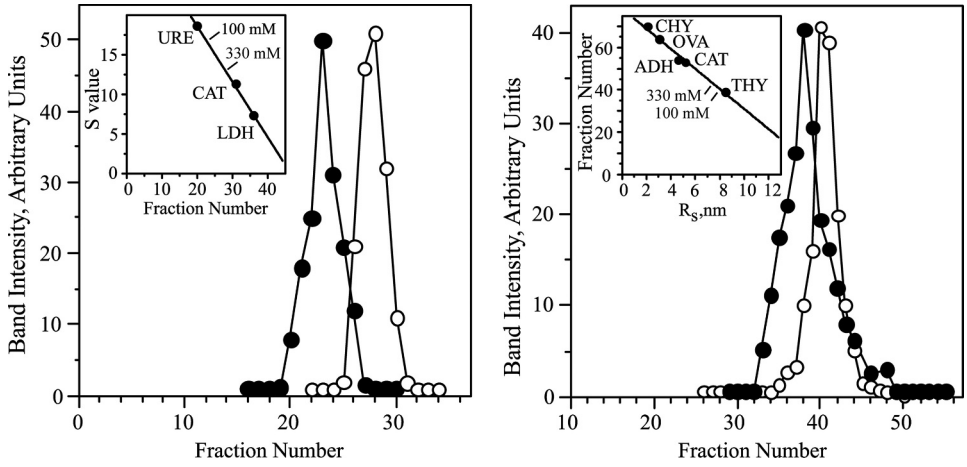

FIGURE 3. **Velocity sedimentation and gel filtration of the human mtDNA helicase in the absence and presence of cofactors.** *Left*, N- and C-terminally His-tagged human mtDNA helicase were sedimented in a 12–30% glycerol gradient as described under "Experimental Procedures." Protein standards run in parallel gradients were: jack bean urease (*URE*, 18.6 S), bovine liver catalase (*CAT*, 11.3 S), and rabbit muscle lactate dehydrogenase (*LDH*, 7.3 S). 330 mM NaCl (*open circles*); 100 mM NaCl in the presence of Mg^{2+}-ATPγS (*closed circles*). *Right*, C-terminally His-tagged human mtDNA helicase was chromatographed on a Superdex 200 HR 10/30 column as described under "Experimental Procedures." Proteins standards used to calibrate the column were: chymotrypsinogen A (*CHY*, R_s = 28 Å), hen egg ovalbumin (*OVA*, R_s = 30 Å), yeast alcohol dehydrogenase (*ADH*, R_s = 46 Å), bovine liver catalase (*CAT*, R_s = 52 Å), and bovine thyroid thyroglobulin (*THY*, R_s = 85 Å). 330 mM NaCl (*open circles*); 100 mM NaCl in the presence of Mg^{2+}-ATPγS/ATP (*closed circles*).

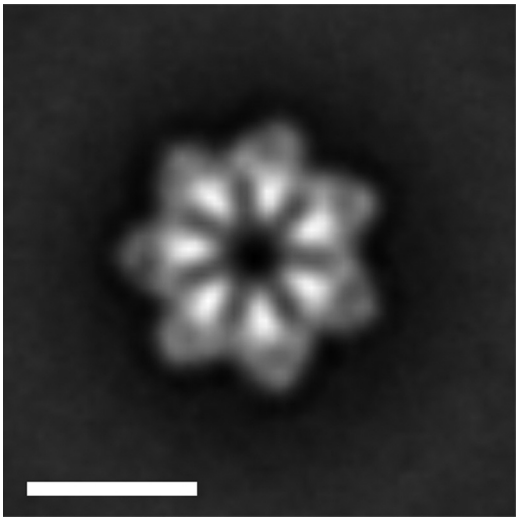

FIGURE 4. **Electron microscopy of the human mtDNA helicase at 100 mM NaCl in the presence of Mg^{2+}-ATPγS.** A representative 7-fold averaged image of the entire population of 4,900 front views is shown. Side views were not observed. The *bar* represents 6 nm. SOM of rotational spectra of the same set of particles is presented in supplemental Fig. S1.

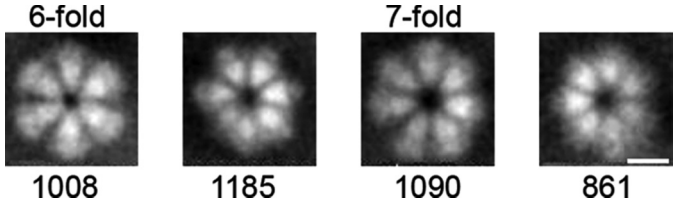

FIGURE 5. **Electron microscopy of the human mtDNA helicase at 150 mM NaCl in the presence of Mg^{2+}-ATPγS.** Class averages obtained by ML2D classification from 4,144 particles. The 6- and 7-fold classes are indicated. The number of particles per class is shown at the *bottom*. The *bar* represents 6 nm. SOM of rotational spectra of the same set of particles is presented in supplemental Fig. S2.

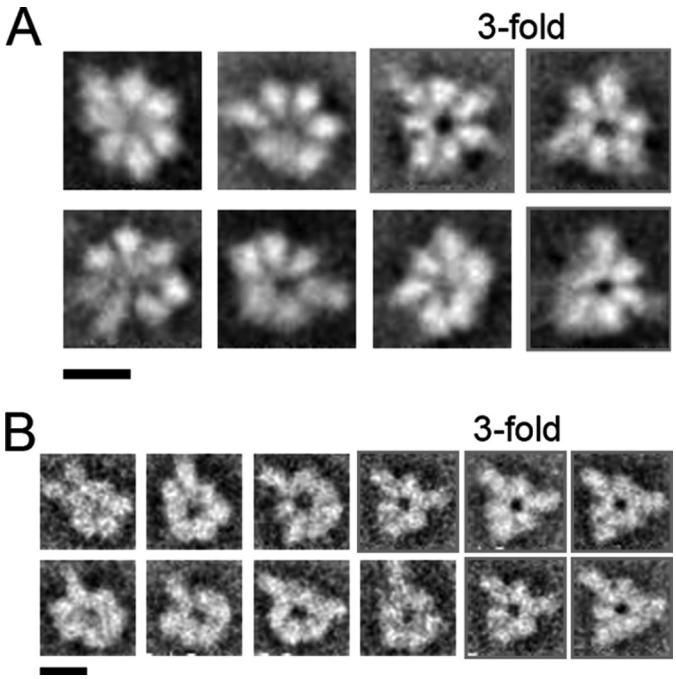

FIGURE 6. **Electron microscopy of the human mtDNA helicase at 330 mM NaCl.** *A*, class averages obtained by ML2D classification applied to a set of 4317 particles. The 3-fold "top view" classes are indicated. *B*, classes resulting from CL2D classification. Some 3-fold classes are indicated. The *bar* represents 10 nm. SOM of rotational spectra of the same set of images are presented in supplemental Fig. S3.

oligomeric state when bound to ATPγS. This estimated native molecular weight corresponds to that of a heptamer.

Examination of Oligomeric States of the Human mtDNA Helicase by Electron Microscopy—To characterize structurally oligomeric states of the human mtDNA helicase observed by glutaraldehyde cross-linking and hydrodynamic methods under various solution conditions, we performed single particle electron microscopy.

100 mM NaCl Plus Cofactors—A total of 4,900 front view particles were extracted from electron micrographs of negatively stained material prepared in 100 mM NaC1 in the presence of 4 mM $MgCl_2$ and 2 mM ATPγS. This set of images was aligned and classified using the maximum-likelihood two-dimensional method (ML2D, (29)) designed to analyze structural heterogeneity of macromolecular complexes. All the classes obtained showed images with a clear 7-fold-symmetry, indicating that this was the predominant form in the image population. A representative averaged image is shown in Fig. 4. The same result was obtained using another classification algorithm based on self-organizing maps of image rotational spectra (SOM, Refs. 30, 32), (supplemental Fig. S1). These two-dimensional analyses indicated that the human mtDNA helicase at 100 mM NaCl in the presence of ATPγS is very homogeneous in structural terms. The most characteristic view (also referred to in this work as the "top view") clearly presents a closed ring with a very pronounced 7-fold symmetry. The ring has an outer ring diameter of 12 nm and an inner channel of ~1 nm inner diameter that is accessible to the negative staining agent.

150 mM NaCl Plus Cofactors—4,144 top views were used in the analysis of the human mtDNA helicase at 150 mM in the presence of 4 mM $MgCl_2$ and 2 mM ATPγS. Both ML2D (Fig. 5) and SOM classification (supplemental Fig. S2) showed a mixture of 7- and 6-fold particles with seven and six density lobes, respectively, organized in a ring. These results indicate that at 150 mM NaCl in the presence of cofactors, the human mtDNA helicase exists as a mixture of two conformations with 6- and 7-fold symmetry. Both methods detected a significant population of tilted or rocking particles, those without defined monomers in ML2D and those with a main component in the harmonic one or two of the rotational spectra. For these particles, it is not possible to determine the exact number of monomers, and for that reason, we cannot quantify precisely the percentage of each of the two classes present in the sample.

330 mM NaCl—A set of 4,317 images was utilized to analyze the structure of the human mtDNA helicase at 330 mM NaCl. The classification of these images using ML2D (Fig. 6*A*) and SOM (supplemental Fig. S3) clearly indicated that the sample exhibited a much larger degree of structural flexibility than the samples analyzed under the low salt conditions. Because of the high degree of structural heterogeneity, the quality of the averaged image obtained is lower than in the low salt buffer conditions. Despite that, we are able to detect particles with a 3-fold symmetry that were not detected in the previous conditions. We obtained a similar structural heterogeneity using other approaches such as CL2D (see "Experimental Procedures" and

Fig. 6*B*) and EMAN (data not shown). These results suggest that the sample at 330 mM NaCl exists in a wider range of conformations than under the low salt conditions, in some cases rendering very elongated and possibly tilted views. In this population we only detect "top views" of 3-fold particles and not of 6- and 7-fold similar to those detected previously. A similar 3-fold quaternary organization has been detected in other DnaB-like hexameric helicases such as DnaB (12) or bacteriophage SPP1 G40P (33), suggesting that the 3-fold "top views" observed correspond to hexameric particles of the human mtDNA helicase.

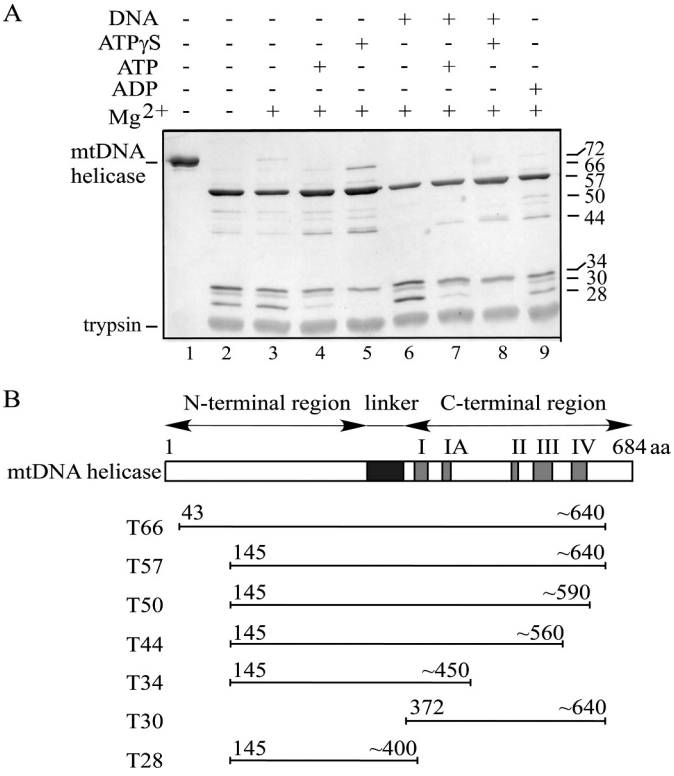

FIGURE 7. **Trypsin digestion of the human mtDNA helicase reveals conformational changes upon cofactor and DNA substrate binding.** *A*, human mtDNA helicase was proteolyzed with trypsin at 100 mM NaCl at 24 °C. Samples were analyzed by SDS-PAGE followed by silver staining. *Lane 1*, undigested helicase; *lane 2*, absence of cofactors; *lane 3*, Mg^{2+} only; *lane 4*, Mg^{2+}-ATP; *lane 5*, Mg^{2+}-ATPγS; *lane 6*, Mg^{2+}-DNA; *lane 7*, Mg^{2+}-ATP-DNA; *lane 8*, Mg^{2+}-ATPγS-DNA; *lane 9*, Mg^{2+}-ADP. DNA refers to heat-denatured DNase I-activated calf thymus DNA (ssDNA length ~300 nt). *B*, schematic diagram of proteolytic fragments of human mtDNA helicase (modified from Ziebarth *et al.* (1)).

Trypsin Digestion of the Human mtDNA Helicase Reveals Conformational/Structural Changes upon Cofactor and DNA Binding—To evaluate the changes induced by the binding of cofactors and DNA, we subjected the mtDNA helicase to limited proteolysis with trypsin at 100 mM NaCl (see "Experimental Procedures"). In the absence of DNA (Fig. 7*A*, *lanes 2–5* and *9*), the presence of Mg^{2+} alone or Mg^{2+}-ADP (*lanes* 3 and *9*, respectively) produces the same pattern of digestion as in the absence of cofactors (*lane* 2), suggesting no conformational or structural changes. However, the addition of ATP or ATPγS (*lanes* 4 and *5*) prevents the production of the characteristic smaller proteolytic products of 28 and 30 kDa (T28 and T30, respectively; Fig. 7*B*) that are typically produced in the absence of cofactors or presence of Mg^{2+} or Mg^{2+}-ADP. We evaluated further the appearance of these species in a time course analysis in the presence of Mg-ATPγS, and found that whereas a faint band corresponding to T28 was produced after 20 min of digestion, T30 was not produced over the entire 90-min time course (data not shown). Thus, in the reaction containing Mg^{2+}-ATP (*lane 4*), the presence of a minor band at the position of T30 likely results from ATP hydrolysis to yield either apoenzyme or enzyme bound to Mg^{2+}-ADP, as in *lanes 2* and *9*, respectively. Our data indicate that NTP binding causes occlusion of trypsin cleavage sites that does not occur upon NDP binding. This occlusion is most likely induced by a structural and/or conformational change in the mtDNA helicase.

Binding of ssDNA induces a different set of changes than does NTP binding. We found that the presence of heat-denatured DNase I-activated calf thymus DNA (or 75-mer oligonucleotide, data not shown) results in the disappearance of the intermediate proteolytic products T50 and T44 (Fig. 7, *lane* 6), while their derivative products T34 and T28 appear to be produced in higher amounts. Binding of Mg^{2+}-ATP or Mg^{2+}-ATPγS in the presence of ssDNA reverses these effects (*lanes* 7 and *8*). To evaluate this further, we performed a DNA titration in the absence or presence of cofactors, followed by trypsin digestion. We found that the digestion patterns are identical in the presence or absence of Mg^{2+} or Mg^{2+}-ADP, and show a decrease in the appearance of T50 and T44 as DNA concentration increases (Fig. 8*A*, *lanes 3–5*; Fig. 8*B*, *lanes 3–8*). Although the decrease in the intermediate products is also observed in the presence of Mg^{2+}-ATPγS (Fig. 8*A*, *lanes 6–8*), its binding clearly renders the enzyme more resistant to proteolysis. The data demonstrate that the mtDNA helicase is capable of binding DNA in the absence of cofactors but its susceptibility to proteolytic digestion, and hence its structural conformation, likely differs in the presence of both DNA and Mg^{2+}-ATPγS.

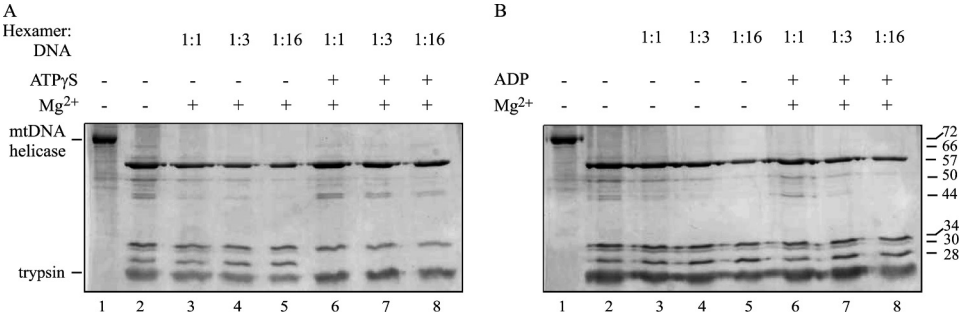

FIGURE 8. **Trypsin digestion of the human mtDNA helicase bound to DNA reveals a proteolytically sensitive conformation.** Human mtDNA helicase was proteolyzed with trypsin at 100 mM NaCl at 24 °C using molar ratios of hexamer: DNA of 1:1, 1:3, and 1:16. Samples were analyzed by SDS-PAGE followed by silver staining. *A*, *lane 1*, undigested helicase; *lane 2*, absence of cofactors; *lanes 3–5*, Mg^{2+} only; *lanes 6–8*, Mg^{2+}-ATPγS. *B*, *lane 1*, undigested helicase; *lanes 2–5*, absence of cofactors; *lanes 6–8*, Mg^{2+}-ADP. DNA refers to heat-denatured DNase I-activated calf thymus DNA (ssDNA length ~300 nt).

DISCUSSION

The fluctuating ionic environment within the matrix of the mito-

chondrion varies in accordance with the metabolic state of the organelle, and is highly likely involved in mitochondrial regulation (34). Our recombinant human mtDNA helicase, however, is purified as a stable, soluble protein only at elevated salt concentrations above 250 mM NaCl (1). At ionic conditions more representative of the mitochondrial environment, we found that in the absence of cofactors such as Mg^{2+} and ADP or ATP, the enzyme is largely insoluble. Higher salt concentrations in concert with increasing temperature result in increased solubility of the human mtDNA helicase. This is consistent with studies of *E. coli* DnaB protein and bacteriophage T4 gene 41 protein that suggest protomer multimerization as temperature or ionic strengths are elevated (9, 11, 35). Mg^{2+} has a moderately stabilizing effect on these proteins, whereas nucleoside diphosphate produced no effect. The mtDNA helicase is most stable when Mg^{2+} is present and NTP is bound, and may suggest cellular interactions that do not require the energy of nucleotide hydrolysis.

Our cross-linking data show that in the absence of glutaraldehyde and cofactors, a dimeric form exists that possesses strong subunit interactions, which are resistant to the conditions of denaturing gel electrophoresis. Thus, the previously described hexamer of the human mtDNA helicase could assemble via a trimerization of dimers, as shown for recombinant forms of bacteriophage T4 gene 41 protein and the simian virus 40 Large T antigen helicase domain (10, 36). We found that with the addition of glutaraldehyde in the absence of cofactors the abundance of multiple oligomeric bands is very low, corroborating our solubility data. Addition of Mg^{2+} and NTP produces a significant increase in band intensity that we interpret as a stabilizing effect on the oligomeric structure, and is consistent with findings on hexameric *E. coli* DnaB (11, 22). We have reported previously that mtDNA helicase exists predominantly as homogeneous hexamers in a buffer containing 330 mM NaCl (1). Electron microscopic analysis under the same conditions indicates that the majority of molecules are hexamers that possess 3-fold symmetry with a high degree of structural flexibility. However, at 100 mM NaCl in the presence of ATPγS, only molecules with 7-fold symmetry corresponding to a heptameric species are observed. The presence of Mg^{2+} and NTP seems to be a crucial factor influencing the oligomeric state of the protein. Furthermore, we have demonstrated by velocity sedimentation and size exclusion chromatography that in the presence of Mg^{2+} and nucleoside triphosphate at low salt concentrations human mtDNA helicase elutes as a single peak, which corresponds to the heptamer. Because both hexameric and heptameric molecules are clearly visible in the electron micrographs obtained at 150 mM NaCl in the presence of NTP, it appears that in the presence of nucleoside triphosphate, lower ionic strength favors heptameric structures. Heptamers have also been identified in T7 gp4, *mt*MCM protein and *T. thermophilus* HB8 RuvB protein, but the biochemical relevance of this state remains elusive (3, 4, 6, 7). It seems unlikely that the hexamers acquire a monomer, because monomers are not detected in sedimentation analysis or by electron microscopy. One possibility is that only heptamers are capable of binding NTP, and any hexamers present aggregate in the low salt environment. This might provide an explanation for the low specific activity of the mitochondrial enzyme in helix unwinding. Unfortunately, we could not explore this salt dependence phenomenon further because the protein is highly insoluble at low salt in the absence of nucleoside triphosphate, and does not bind nucleotides at elevated ionic strengths.

We could however evaluate the influence of the cofactors on the oligomeric structure of the human mtDNA helicase in limited proteolysis experiments, which require only a transient exposure of the enzyme to lower salt conditions. Proteolysis of the helicase with trypsin produces seven prominent cleavage products: T66, T57, T50, T44, T34, T30, and T28. We have shown previously that the initial trypsin product, T66, represents a human mtDNA helicase lacking its C terminus (1). A subsequent cleavage at the N terminus at residue Lys-144 produces T57. The progressive cleavage of T57 at its C terminus gives rise to T55, T44, T34 and the minimal fragment T28. Fragment T30 is unique as it does not share a common N terminus with the derivatives of T50, T44, T34, and T28; it is produced from cleavage of T57 at residue Arg-371, and represents a minimal C-terminal domain. In the trypsin digestion experiments presented here, proteolysis in the presence of NTP results in the loss of T30. This loss is not associated with nucleotide binding in general because this effect is not observed in the presence of ADP. Rather, it seems evident that the enzyme undergoes a structural and/or conformational change in the presence of NTP. Our current data support the conclusion that this change is most likely a switch from a hexameric to a heptameric form. By analogy to bacteriophage T7 gp4 protein, a heptameric species would possibly have a larger diameter and a more flat and symmetric structure, which could result in conformation that prevents the formation of T30 upon proteolysis. In our previous proteolytic and functional studies, we proposed that the human mtDNA helicase has an asymmetric subunit orientation within the hexamer, and we speculated that the production of the T30 fragment was a direct result of that asymmetry (1). Consequently, another explanation for the loss of T30 when NTP is bound is a conformational switch in subunit orientation. Such a conformational change would be consistent with the changes observed for other replicative helicases such as *E. coli* DnaB protein, T7 gp4 and bacteriophage T4 gene 41 protein that facilitates the interactions of the proteins with ssDNA (17, 18, 22, 35). In fact, a third possibility is that both a structural and conformational change is occurring simultaneously.

Trypsin proteolysis experiments in the presence of ssDNA reveal that DNA binding can occur in the complete absence of cofactors (Fig. 7 and data not shown). This finding is similar to that observed with the *mt*MCM protein, but contrasts with the nucleotide-dependent DNA binding of *E. coli* DnaB protein and T7 gp4 (16, 22, 23, 37). Our data show that DNA binding leads to a change in the relative abundance of various proteolytic products as evident in the disappearance of T50 and T44, and increases in T34 and T28. Because ssDNA binding can occur in the absence of cofactors, conditions that appear to favor the existence of hexameric structures, we speculate that the hexamers have the ability to bind ssDNA. The ssDNA: hexamer interaction may alter the conformation of the hexamer, changing its sensitivity to proteolysis. In the presence of NTP,

and thus when heptameric species are present, changes in the relative abundance of the proteolytic products are much less pronounced. It seems plausible that the heptamers may bind DNA in an orientation that is different from that of hexamers. What is the biological role of the heptameric species of the human mtDNA helicase? It was suggested that the expanded ring and dimensions of the central channel of the heptameric form of bacteriophage T7 gp4 protein were suitable for accommodating dsDNA (4). However, Crampton *et al.* (3) have recently reported that no DNA binding by the T7 gp4 heptamer was observed by nondenaturing polyacrylamide gel electrophoresis. Unfortunately, despite multiple attempts under various conditions, we were not able to resolve the human enzyme using native polyacrylamide gel electrophoresis, so we could not examine the DNA binding properties of hexamers *versus* heptamers using a similar approach.

Farge *et al.* (38) tested the effects of cofactors on binding of 15, 30 and 45 nt oligomers and their double-stranded forms to the human mtDNA helicase using a gel electrophoretic mobility shift analysis. They observed that the mtDNA helicase binds dsDNA in the complete absence of cofactors. However, they observed binding of the ssDNA 30 mer only in the presence of Mg and ATP or ATPγS. They also found that the mtDNA helicase could not interact with a shorter ssDNA probe (15 mer) under any condition. In our case, we began our limited proteolysis experiments with DNase I-activated calf thymus DNA, and found that the mtDNA helicase binds both the native and heat-denatured forms in the absence of cofactors. Here, we determined the average length of the denatured ssDNA to be ~300 nt. In experiments not shown, we repeated the study with ssDNA oligomers of 15, 18, 22, 38, 45, 60, 75, and 95, and found that binding to the 15–22 mers occurred only in the presence of cofactors and was highly concentration dependent (*i.e.* weak affinity); the 38–60 mers were bound efficiently in the presence of cofactors, but not in their absence, and the 75 and 95 mers were bound efficiently in the presence or absence of cofactors. Thus, we can speculate that the binding of cofactors induces conformational and/or structural changes in the enzyme that facilitate helicase: DNA interactions, and that the DNA length plays an important role.

The human mtDNA helicase has a prokaryotic ancestry that is apparent by its sequence similarity and biochemical characteristics shared with T7 gp4. However, our current data argue that it also resembles eukaryotic and other viral helicases, and suggest both physical and functional diversity. Similarly, archaeal organisms share genetic characteristics with both eubacterial and eukaryotic systems, and although their proteins are more related in sequence to eubacteria, their cellular functions are more similar to eukaryotic processes (39, 40). It is reasonable to assume that the endosymbiotic event that resulted in the establishment of the mitochondrion as a critical eukaryotic organelle drove the evolution of the mtDNA helicase from an ancestral prokaryotic protein toward adoption of mechanistic features more reminiscent of its eukaryotic host, thereby creating a more efficient cellular machine. Thus, we must look beyond the bacteriophage and bacterial model systems for insight in developing experimental approaches to probe the importance of this novel helicase in mitochondrial biogenesis.

Acknowledgments—We thank Roberto Marabini, Sjors Scheres, and Carlos Oscar Sánchez-Sorzano for technical help in the image analysis. We thank Marcos Oliveira for his comments and suggestions during the course of this work, and Marcos Oliveira and Magdalena Felczak for critical reading of the manuscript.

REFERENCES

1. Ziebarth, T. D., Farr, C. L., and Kaguni, L. S. (2007) *J. Mol. Biol.* **367,** 1382–1391
2. Korhonen, J. A., Gaspari, M., and Falkenberg, M. (2003) *J. Biol. Chem.* **278,** 48627–48632
3. Crampton, D. J., Ohi, M., Qimron, U., Walz, T., and Richardson, C. C. (2006) *J. Mol. Biol.* **360,** 667–677
4. Toth, E. A., Li, Y., Sawaya, M. R., Cheng, Y., and Ellenberger, T. (2003) *Mol. Cell* **12,** 1113–1123
5. Crampton, D. J., Mukherjee, S., and Richardson, C. C. (2006) *Mol. Cell.* **21,** 165–174
6. Miyata, T., Yamada, K., Iwasaki, H., Shinagawa, H., Morikawa, K., and Mayanagi, K. (2000) *J. Struct. Biol.* **131,** 83–89
7. Yu, X., VanLoock, M. S., Poplawski, A., Kelman, Z., Xiang, T., Tye, B. K., and Egelman, E. H. (2002) *EMBO Rep.* **3,** 792–797
8. Costa, A., and Onesti, S. (2008) *Biochem. Soc. Trans.* **36,** 136–140
9. Arai, K., Yasuda, S., and Kornberg, A. (1981) *J. Biol. Chem.* **256,** 5247–5252
10. Dong, F., Gogol, E. P., and von Hippel, P. H. (1995) *J. Biol. Chem.* **270,** 7462–7473
11. Bujalowski, W., Klonowska, M. M., and Jezewska, M. J. (1994) *J. Biol. Chem.* **269,** 31350–31358
12. San Martin, M. C., Stamford, N. P., Dammerova, N., Dixon, N. E., and Carazo, J. M. (1995) *J. Struct. Biol.* **114,** 167–176
13. Yu, X., Jezewska, M. J., Bujalowski, W., and Egelman, E. H. (1996) *J. Mol. Biol.* **259,** 7–14
14. Bird, L. E., Håkansson, K., Pan, H., and Wigley, D. B. (1997) *Nucleic Acids Res.* **25,** 2620–2626
15. Patel, S. S., and Hingorani, M. M. (1993) *J. Biol. Chem.* **268,** 10668–10675
16. Picha, K. M., and Patel, S. S. (1998) *J. Biol. Chem.* **273,** 27315–27319
17. Nakayama, N., Arai, N., Kaziro, Y., and Arai, K. (1984) *J. Biol. Chem.* **259,** 88–96
18. Yong, Y., and Romano, L. J. (1995) *J. Biol. Chem.* **270,** 24509–24517
19. Egelman, E. H., Yu, X., Wild, R., Hingorani, M. M., and Patel, S. S. (1995) *Proc. Natl. Acad. Sci. U.S.A.* **92,** 3869–3873
20. Sawaya, M. R., Guo, S., Tabor, S., Richardson, C. C., and Ellenberger, T. (1999) *Cell* **99,** 167–177
21. Singleton, M. R., Sawaya, M. R., Ellenberger, T., and Wigley, D. B. (2000) *Cell* **101,** 589–600
22. Arai, K., and Kornberg, A. (1981) *J. Biol. Chem.* **256,** 5260–5266
23. Matson, S. W., and Richardson, C. C. (1985) *J. Biol. Chem.* **260,** 2281–2287
24. Chong, J. P., Hayashi, M. K., Simon, M. N., Xu, R. M., and Stillman, B. (2000) *Proc. Natl. Acad. Sci. U.S.A.* **97,** 1530–1535
25. Wang, Y., Farr, C. L., and Kaguni, L. S. (1997) *J. Biol. Chem.* **272,** 13640–13646
26. Laemmli, U. K. (1970) *Nature* **227,** 680–685
27. Sorzano, C. O., Marabini, R., Velázquez-Muriel, J., Bilbao-Castro, J. R., Scheres, S. H. W., Carazo, J. M., and Pascual-Montano, A. (2004) *J. Struct. Biol.* **148,** 194–204
28. Scheres, S. H., Núñez-Ramírez, R., Sorzano, C. O., Carazo, J. M., and Marabini, R. (2008) *Nat. Protoc.* **3,** 977–990
29. Scheres, S. H., Valle, M., Nuñez, R., Sorzano, C. O., Marabini, R., Herman, G. T., and Carazo, J. M. (2005) *J. Mol. Biol.* **348,** 139–149
30. Pascual-Montano, A., Donate, L. E., Valle, M., Bárcena, M., Pascual-Marqui, R. D., and Carazo, J. M. (2001) *J. Struct. Biol.* **133,** 233–245
31. Ludtke, S. J., Baldwin, P. R., and Chiu, W. (1999) *J. Struct. Biol.* **128,** 82–97
32. Marabini, R., and Carazo, J. M. (1994) *Biophys. J.* **66,** 1804–1814

33. Bárcena, M., Martín, C. S., Weise, F., Ayora, S., Alonso, J. C., and Carazo, J. M. (1998) *J. Mol. Biol.* **283,** 809–819
34. Hackenbrock, C. R. (1968) *Proc. Natl. Acad. Sci. U.S.A.* **61,** 598–605
35. Liu, C. C., and Alberts, B. M. (1981) *J. Biol. Chem.* **256,** 2813–2820
36. Li, D., Zhao, R., Lilyestrom, W., Gai, D., Zhang, R., DeCaprio, J. A., Fanning, E., Jochimiak, A., Szakonyi, G., and Chen, X. S. (2003) *Nature* **423,** 512–518
37. Kelman, Z., Lee, J. K., and Hurwitz, J. (1999) *Proc. Natl. Acad. Sci. U.S.A.* **96,** 14783–14788
38. Farge, G., Holmlund, T., Khvorostova, J., Rofougaran, R., Hofer, A., and Falkenberg, M. (2008) *Nucleic Acids Res.* **36,** 393–403
39. Edgell, D. R., and Doolittle, W. F. (1997) *Cell* **89,** 995–998
40. Woese, C. R., Kandler, O., and Wheelis, M. L. (1990) *Proc. Natl. Acad. Sci. U.S.A.* **87,** 4576–4579